Received: 4 January 2019 | Accepted: 8 May 2019

DOI: 10.1111/jvim.15526

Journal of Veterinary Internal Medicine Open Access

ACVIM American College of Veterinary Internal Medicine

CASE REPORT

Conventional and functional magnetic resonance imaging features of late subacute cortical laminar necrosis in a dog

Neringa Alisauskaite[1] | Adriano Wang-Leandro[2] | Matthias Dennler[2] | Marta Kantyka[3] | Simone K. Ringer[3] | Frank Steffen[1] | Katrin Beckmann[1]

[1]Neurology Service, Department of Small Animal Surgery, Vetsuisse-Faculty Zurich, Zurich, Switzerland

[2]Clinic for Diagnostic Imaging, Department of Diagnostics and Clinical Services, Vetsuisse-Faculty Zurich, Zurich, Switzerland

[3]Clinic for Anesthesia, Department of Diagnostics and Clinical Services, Vetsuisse-Faculty Zurich, Zurich, Switzerland

Correspondence
Neringa Alisauskaite, Vetsuisse Faculty, University of Zurich, Winterthurerstrasse 260, 8057 Zurich, Switzerland.
Email: nalisauskaite@vetclinics.uzh.ch

Abstract

Cerebral cortical laminar necrosis (CLN) is a consequence of severe hypoxic, ischemic, or hypoglycemic events. In humans, these cortical lesions show characteristic linear T1-weighted (T1W) hyperintensity in the late subacute stage. Limited information reporting magnetic resonance imaging (MRI) findings in dogs affected by CLN is available. A 3-year-old Belgian Shepherd dog was referred 8 days after sudden onset of blindness after general anesthesia. Neurological examination showed central blindness and mild ataxia. Three-Tesla MRI examination of the brain revealed bilateral asymmetrical areas of T2-weighted hyperintensity within the occipital, parietal, temporal, and frontal cortex, involving gray and white matter. Furthermore, linear T1W-hyperintense lesions were found in the cerebral cortex of the same areas and showed heterogeneous contrast enhancement. Perfusion-weighted images revealed hyperperfusion in the affected regions. Lesions were compatible with subacute CLN with corresponding edema suspected to be secondary to anesthesia-related brain hypoxia. Three-Tesla MRI enabled identification of the laminar pattern of the cortical lesions.

KEYWORDS

arterial spin labeling, brain perfusion, cerebral hypoxia, polioencephalomalacia

1 | INTRODUCTION

Cortical laminar necrosis (CLN), a selective polioencephalomalacia, displays laminar distribution in the cerebrocortical gray matter.[1,2] High metabolic rate and therefore higher perfusion demand make the cerebral cortex highly susceptible to ischemic, hypoxic, and metabolic events that might compromise cerebral perfusion.[3] In humans, pathognomonic T1-weighted (T1W) hyperintense lesions after the gyral anatomy of the cerebral cortex characterize CLN in magnetic resonance imaging (MRI).[2,4,5] These curvilinear T1W hyperintensities follow a temporal course appearing few days to 2 weeks after the event.[1,2,5] The T1W hyperintensities typically are most pronounced 1 month after the cerebral perfusion compromise and fade out over the following 3 to 11 months.[1,2,6] Cortical T1W-increased signal intensity (SI) in nonhemorrhagic lesions occurs most likely because of increased mobility of proteins or lipid accumulation in macrophages.[1,5,7]

In dogs, CLN occurs secondary to hypoxia, hypoglycemia, fluid overload, smoke inhalation, ischemic stroke, encephalitis, and prolonged seizure activity, being diagnosed mostly through postmortem histopathologic examinations.[8-15] Magnetic resonance imaging characterization of CLN in dogs is limited and comprises examinations

Abbreviations: ADC, apparent diffusion coefficient; ASL, arterial spin labeling; CBF, cerebral blood flow; CLN, cortical laminar necrosis; CSF, cerebrospinal fluid; DWI, diffusion-weighted imaging; FLAIR, fluid-attenuated inversion recovery; MRI, magnetic resonance imaging; pCASL, pseudo-continuous arterial spin labeling; PWI, perfusion-weighted imaging; ROI, region of interest; SI, signal intensity; T1W, T1 weighted; T2W, T2 weighted; TE, echo time; TR, repetition time.

performed with low-field and in 1 case with high-field 1.5-Tesla MRI scanners.[8,13,14]

In human medicine, diffusion-weighted imaging (DWI) and perfusion-weighted imaging (PWI) are commonly utilized for ischemic, hypoxic, or both brain lesion characterization.[16-19] Diffusion-weighted imaging, including apparent diffusion coefficient (ADC) maps, allows more accurate identification of regions with restricted diffusion compared to conventional MRI sequences.[16,17,20] Perfusion-weighted imaging enables evaluation of cerebral blood flow (CBF) with a broad spectrum of applications, including detection of hypoperfused brain areas after hypoxic and ischemic events, evaluation of the extent of parenchymal damage, and monitoring of the temporal course of cerebral perfusion patterns after global anoxic events.[21-23] Arterial spin labeling (ASL), a noninvasive PWI technique, facilitates quantitative and accurate measurement of the CBF using intravascular water as an endogenous contrast agent.[22]

In the current case report, we present the 3-Tesla MRI features, including brain diffusion and perfusion evaluation, of CLN in a Belgian Shepherd dog after general anesthesia.

2 | CASE PRESENTATION

A client-owned 3-year-old, 37 kg, male intact, working police Belgian Shepherd Malinois dog was presented at the neurology service in the small animal clinic of the University of Zurich. The dog had a history of a dental procedure by a private veterinarian 8 days before presentation. Based on the information obtained from the private veterinarian, the dog was sedated with 0.005 mg/kg medetomidine, 0.006 mg/kg buprenorphine, and 0.013 mg/kg acepromazine, all given intramuscularly at once. Anesthesia was induced with propofol (dose unknown) and maintained with isoflurane in oxygen air mix. Ringer's acetate infusion (7 mL/kg/h) was used during anesthesia. Instituted monitoring consisted of the heart rate, electrocardiogram, pulse oximetry, and inspired and expired carbon dioxide and oxygen. No complications in the peri-anesthetic period were reported; all measurements stayed within reference range according to the provided information; however, no paper record of anesthesia was provided. The procedure lasted for about 60 minutes. At the end of anesthesia, atipamezole at unknown dose was administered. No blood pressure monitoring or inhaled anesthetic concentration was measured. After anesthesia, the dog showed transient excitation and vocalization for 1.5 hours and was bilaterally blind. Subsequently, infusion treatment with Ringer's acetate infusion was initiated and the dog was discharged 1 day later. As vision had not recovered within 1 week after anesthesia, the case was referred for further examinations to the University of Zurich.

At presentation, abnormalities were not detected in the clinical examination, and the neurological examination revealed bilateral blindness with normal direct and indirect pupillary light reflex and generalized proprioceptive ataxia. Therefore, the neuroanatomic localization was the forebrain with postchiasmatic central blindness. Blood biochemistry revealed increased alanine amino transferase activity of 120 U/l (reference range, 20-93). Hematology results showed thrombocytopenia of 120 – 10^3 cells/μL (reference range, 130-394), microcytosis with mean corpuscular volume of 62 fL (reference range, 64-73), and reduced mean corpuscular hemoglobin of 22 pg (reference range, 23-26). Otherwise, blood examination results did not reveal any abnormalities, and the dog was scheduled for MRI under general anesthesia the same day. Sedation consisting of 0.2 mg/kg butorphanol and 0.007 mg/kg acepromazine was administered IV. Anesthesia was induced with propofol dosed to effect. Maintenance of anesthesia was with sevoflurane in oxygen and medical air. Normocapnia was maintained using intermittent positive pressure ventilation. Ringer's acetate was administered at a rate of 2.5 mL/kg/h. End-tidal concentration of sevoflurane, heart rate, noninvasive monitoring of blood pressure, arterial oxygen saturation, and end-tidal carbon dioxide were monitored using a multiparameter monitor (Datex Ohmeda, Madison, Wisconsin). Initial mild hypotension (mean arterial blood pressure of 55 mm Hg) was treated with an intravenous bolus (7 mL/kg) of Ringer's acetate and dobutamine constant rate infusion (titrated from 2 mcg/kg/min till up to 5 mcg/kg/min). Dobutamine improved mean arterial blood pressure till 60 mm Hg, but as suspicion of vasodilation was made based on short capillary refill time of 0.5 seconds, it was switched to dopamine (7 mcg/kg/min). The dog stayed normotensive through the procedure. Medetomidine (0.5 mcg/kg) was administered IV before recovery to prevent emergence delirium.

Magnetic resonance imaging of the brain was performed with a 3-Tesla MRI scanner (Philips Ingenia, Philips AG, Zurich, Switzerland) using a 20-channel head/neck coil. The dog was positioned in dorsal recumbency and the scanning protocol included spin echo transverse, sagittal, and dorsal T2W (repetition time [TR] 2753-5030 ms; echo time [TE] 100 ms; slice thickness 2.5-2.8 mm), transverse fluid attenuation inversion recovery (FLAIR) (TR 11000 ms; TE 125 ms; slice thickness 2.8 mm), and gradient echo pre- and post-contrast 3D T1W images (TR 11 ms; TE 5.1 ms; slice thickness 0.7 mm) images. In addition, transverse DWI (TR 3914 ms; TE 98 ms; slice thickness 2 mm) was performed and ADC map was produced. For post-contrast image acquisition, gadopentetate dimeglumine (0.1 mmol/kg; Omniscan, GE Healthcare AG, Opfikon, Switzerland) contrast medium was administered intravenously.

Perfusion-weighted images were acquired using 3D pseudo-continuous arterial spin labeling (3D pCASL) imaging sequence (TR 4295 ms; TE 15 ms; slice thickness 6 mm). Labeling stack and slices were oriented perpendicular to the carotid arteries of the dog; furthermore, the post-labeling delay was set at 1950 ms. Images were transferred to a workstation and analyzed using a commercially available software (IntelliSpace Portal; version 7.0). Cerebral blood flow maps were generated and registered to anatomical T1W images. Subsequently, regions of interest (ROIs) measuring blood flow (mL blood/100 g tissue per minute) were placed in the following brain areas: gray matter of the frontal cortex and associated white matter at the level of caudate nucleus in the coronal gyrus next to the coronal sulcus, gray matter of the parietal cortex at the level of mesencephalon in the marginal gyrus, and gray matter of the occipital cortex and associated white matter at the level of the fourth ventricle in the marginal gyrus (Figure 1). Cerebral blood flow values derived from the abovementioned ROIs are summarized in Table 1.

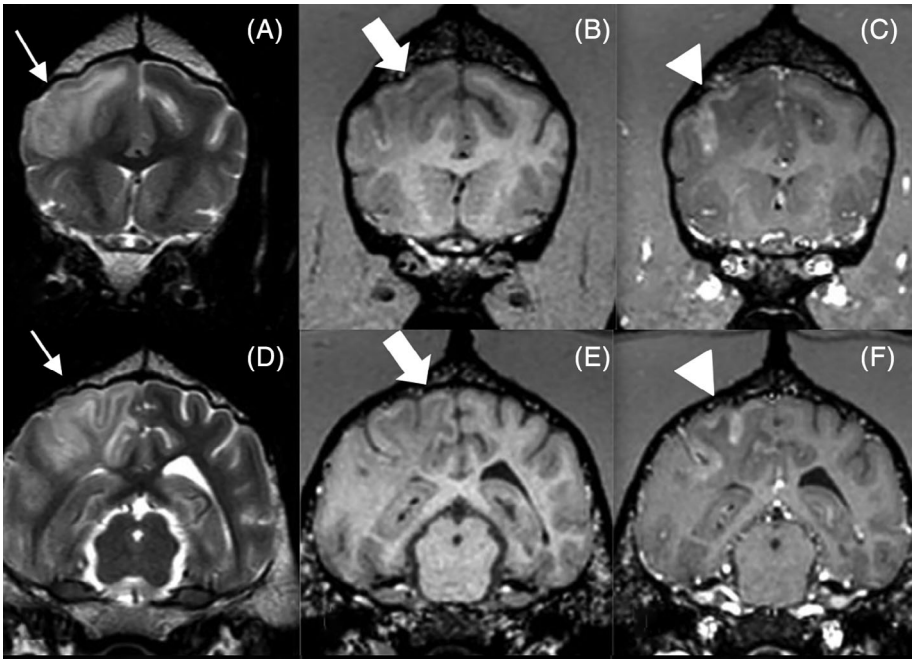

FIGURE 1 Three-Tesla magnetic resonance imaging (MRI) of the brain of the dog suffering consequences of a suspected hypoxic event. Areas of T2 weighted (T2W) increased signal intensity (SI) within the A, frontal and D, parietal cortex, involving gray and white matter (thin arrows). Linear T1 weighted (T1W) increased SI lesions in the cerebral cortex in the B, frontal and E, parietal cortex (thick arrows), undergoing moderate heterogeneous contrast enhancement (C, F, arrowheads). Magnetic resonance images are displayed in a standard fashion (right/left)

TABLE 1 Cerebral perfusion values in affected cerebral areas with abnormal T1-weighted (T1W) pre-/post-contrast and T2-weighted (T2W) signal intensity (SI), in areas of apparently normal brain in the contralateral hemisphere and in the corresponding brain areas of the control dog

Regions of interest (ROIs)	T2W	Pre-contrast T1W	T1W contrast enhancement	CBF in affected brain areas (mL blood/100 g tissue per minute)	CBF in apparently normal brain areas (mL blood/100 g tissue per minute)	CBF in healthy Beagle brain (mL blood/100 g tissue per minute; values in right/left hemispheres)
White matter associated with the frontal cortex at the level of caudate nucleus in the coronal gyrus[a]	Hyper	Hypo	No	45.6	14.9	13.6/14.4
Gray matter of the frontal cortex at the level of caudate nucleus in the coronal gyrus[b]	Hyper	Hyper	Yes, strong	79.8	19.8	31/30.3
Gray matter of the parietal cortex at the level of mesencephalic aqueduct in the marginal gyrus[c]	Hyper	Hyper	Yes, mild	67.7	35.7	20.8/22.8
White matter associated with the occipital cortex at the level of the fourth ventricle in the marginal gyrus[d]	Hyper	Hypo	No	53.0	11.0	11.0/9.0
Gray matter of the occipital cortex at the level of the fourth ventricle in the marginal gyrus[e]	Hyper	Hyper	Yes, strong	72.5	28.9	18.1/18.1

Abbreviations: CBF, cerebral blood flow; Hyper, increased SI compared to cerebral gray matter; Hypo, decreased SI compared to cerebral gray matter.
[a]Region of interest marked as red ellipse in Figure 3.
[b]Region of interest marked as black ellipse in Figure 3.
[c]Region of interest marked as green ellipse in Figure 3.
[d]Region of interest marked as dark red ellipse in Figure 3.
[e]Region of interest marked as light blue ellipse in Figure 3.

A cisternal cerebrospinal fluid (CSF) tap was performed in aseptic conditions after the MRI investigation.

Moreover, 3D T1W and pCASL sequences from a 3-year-old intact female healthy Beagle (same imaging acquisition and slightly different anesthesia protocol using butorphanol, propofol, and sevoflurane), archived from an independent research study (animal permission number ZH272/16), were used for comparison. During postprocessing, ROIs were placed in the same brain areas as in the investigated dog (Table 1).

Magnetic resonance imaging examination of the brain of the affected dog revealed bilateral asymmetrical areas of increased T2

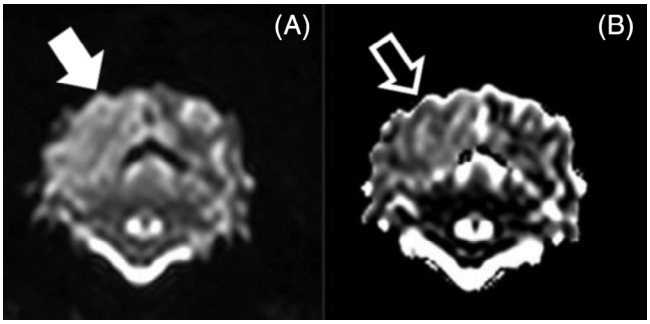

FIGURE 2 Three-Tesla diffusion-weighted magnetic resonance (MR) images of the occipital area of the brain of the dog suffering consequences of a suspected hypoxic event. Presence of increased signal intensity (SI) in diffusion-weighted imaging (DWI) (A, arrow) and apparent diffusion coefficient (ADC) map (B, empty arrow) demonstrating unrestricted diffusion in the affected cortical gray matter. Magnetic resonance images are displayed in a standard fashion (right/left)

and FLAIR SI within the occipital, parietal, temporal, and frontal cortex and associated white matter compared to spared forebrain areas. Furthermore, linear T1W-hyperintense lesions were found in the cerebral cortex of the same areas that underwent moderate heterogeneous enhancement after contrast-medium administration. The affected areas caused a mild mass effect on the surrounding tissues, mildly compressing the right lateral ventricle, and displacing the midline. The affected areas displayed increased SI in DWI sequences and ADC maps (Figure 2).

In pCASL sequence, color-coded maps and CBF values evidenced increased perfusion in the gray and white matter of the right hemisphere at the occipital, parietal, temporal, and frontal lobes (Figure 3; Table 1). Magnetic resonance imaging diagnosis was a severe, asymmetric, diffuse, and multifocal intra-axial lesion affecting mostly the cerebral cortex and subcortical white matter. The lesions were compatible with subacute laminar cortical necrosis with corresponding edema suspected to be secondary to anesthesia-related brain hypoxia.

Cerebrospinal fluid examination did not reveal any abnormalities.

The dog was euthanized few days after the examination on owner's request because of persisting blindness. Consent for post-mortem examination was not available.

3 | DISCUSSION

In the current case presentation, 3-Tesla MRI findings in a dog with CLN secondary to suspected anesthesia related brain hypoxia are reported. Magnetic resonance imaging findings in the current case presentation are similar to the 1.5-Tesla MRI findings described in another case presentation, where increased cortical SI was detected in T2W, pre-, and post-contrast T1W MR images in a dog after status epilepticus.[8] Cortical linear T1W hyperintensity in MR images, pathognomonic for CLN in humans,[1,2,7,24] has not been described in any other veterinary report investigating diagnostic imaging features of CLN in dogs. This could be

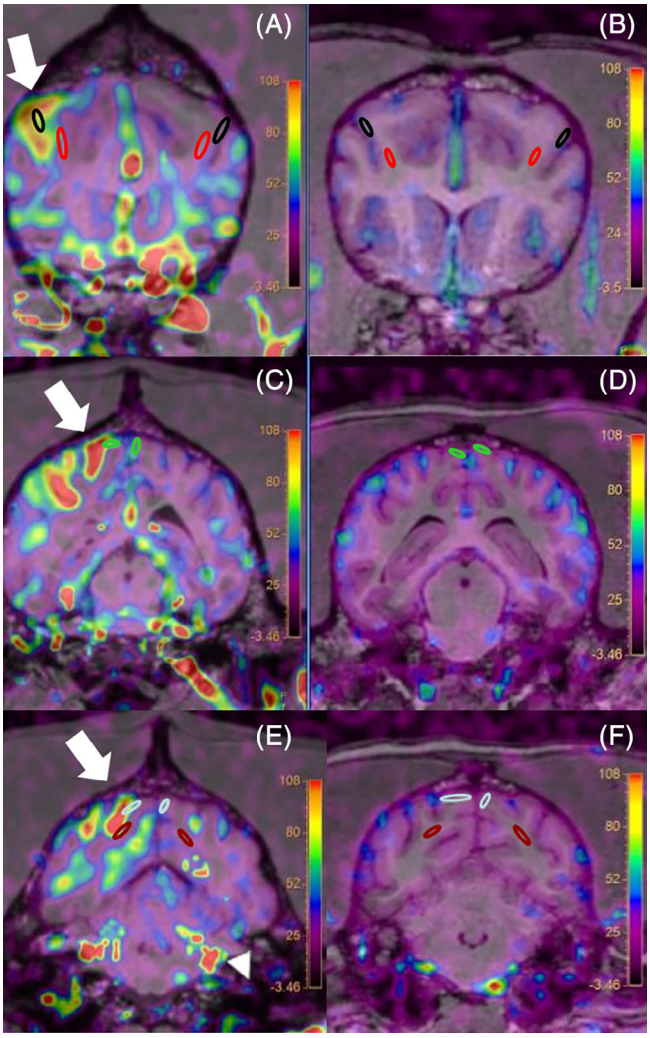

FIGURE 3 Cerebral blood flow (CBF) maps and region of interest (ROI) positioning in the brain of the dog suffering consequences of a suspected hypoxic event (A, C, E) and in a control dog (B, D, F). In the color-coded CBF maps areas corresponding to abnormal signal intensity (SI) in T1-weighted (T1W), T2-weighted (T2W), and diffusion-weighted imaging (DWI) images display increased perfusion (arrows) in frontal (A), parietal (C), and occipital (E) cortex. Regions of interest were placed in the CBF maps within the gray (A, black ellipses) and white (A, red ellipses) matter of the affected right hemisphere and apparently normal parenchyma in the left hemisphere frontal cortex in the dog affected by cortical laminar necrosis (CLN) and in the control dog (B, red and black ellipses), in the parietal cortex in the dog affected by CLN (C, green ellipses), in the control dog (D, green ellipses), in the occipital cortex gray (E, light blue ellipses) and white (E, dark red ellipses) matter in the dog affected by CLN, and in the control dog (F, light blue and dark red ellipses). Images are displayed in a standard fashion (right/left)

attributed to the magnetic field strength, as low-field MRI was used in most of the previous investigations, precluding identification of subtle cortical changes.[11-13] In the current and another case report, dogs were scanned 8 days after the suspected hypoxic event and linear T1W hyperintensity was detected.[8] Although cortical linear T1W increased SI in humans appears at the late subacute stage (7-28 days) after a hypoxic

TABLE 2 Temporal course of the magnetic resonance imaging (MRI) signal intensity (SI) changes in the affected cortical gray matter compared to normal brain SI in cases of cerebral cortical necrosis in humans, modified from refs. [1,2,5]

	Cerebral cortex		
Temporal phase	T2W	Pre-contrast T1W	Contrast enhancement
Hyperacute (≤1 day) and acute (1-3 days)	Iso/Hyper	Iso/Hypo	No
Early subacute (3-7 days)	Iso/Hyper	Iso/Mildly hyper	Yes/No
Late subacute (7-14 [28] days)	Hyper	Iso/Mildly hyper	Yes
Chronic (>14 [28] days)	Hyper	Hyper	Yes

Abbreviations: Hyper, increased SI compared to cerebral gray matter; Hypo, decreased SI compared to cerebral gray matter; Iso, equal SI compared to cerebral gray matter; T2W, T2 weighted.

and ischemic events, the T1W hyperintensity commonly starts to be visible in 2 weeks and is most pronounced 4 weeks after the event (Table 2), whereas in both cases in dogs linear T1W hyperintensity was well pronounced already at day 8.[1,5,8] This suggests that the temporal course might be slightly different in dogs compared to humans. Brain lesions after hypoxic event in another case report were bilateral and symmetrical, but typically asymmetrical lesion distribution is observed in dogs and humans affected by global cerebral ischemia.[1,2,8,12]

Similar brain areas (mainly occipital and parietal) have been confirmed to be affected in MRI examinations in the investigated dog and in other dogs.[8,11-13] Cortical laminae 3 and 5, containing pyramidal neurons, are more susceptible to ischemic and hypoxic damage and are commonly affected in humans.[25] Various cortical layers are damaged in dogs, in most cases lamina 3 being affected in combination with different other layers.[8,13,15,26] It is thought that neurons in certain cortical areas and laminae are more vulnerable because of a higher metabolic demand, higher concentration of excitatory glutamate receptors, and increased vulnerability to oxygen-free radical-induced cell damage, leading to intracellular calcium accumulation.[27-29]

Associated with the lesions in the cerebral cortex, additional white matter signal changes were visible in the case presented here (Figure 1). In agreement with reports from human patients, white matter lesions beneath cortical areas damaged by hypoxic, ischemic, or both events were detected in the acute stage after suspected global brain ischemia in a dog.[5,7,12] In humans affected by CLN, white matter changes detected on MRI appear approximately 1 month after the hypoxic events and tend to increase with time.[5,7] In humans, increased T2W SI in the white matter is explained by myelin degeneration process at the chronic stage after anoxic events because of decreased blood flow, which could be the case in the present case report, only with faster lesion development.[5,7] On the other hand, these white matter changes were not observed neither in MRI nor in a postmortem examination in 2 dogs examined in the chronic phase.[8,12] It could represent vasogenic, cytotoxic edema, or both at the acute and subacute phase in dogs (Figures 1 and 2).[12] Another potential explanation could be the oligodendrocyte resistance to damage in dogs compared to humans.

Signal intensity of the lesions was increased in both DWI sequence and ADC map (Figure 2). In contrast to the acute stage of cerebral stroke, increased SI in DWI and ADC maps has been recognized in humans affected by ischemic lesions during the subacute stage.[30] Therefore, findings in the presented dog are compatible with findings in human DWI of subacute CLN.

An increased perfusion pattern was recognized in the dog affected by CLN in the CBF map, visually and quantitatively, predominantly in the right hemisphere. Cerebral blood flow values derived from affected brain areas were higher in comparison to apparently normal brain parenchyma of the contralateral hemisphere and in the same brain areas of a healthy Beagle dog (Table 1). This finding suggests evolvement of the lesion to brain hyperperfusion, which is a well-recognized phenomenon in humans several days after a hypoxic event.[21,23,31] Hyperperfusion in the subacute stage after cerebral ischemia is explained by loss of vascular autoregulation.[21,32] Early stage cerebral hyperperfusion is associated with ongoing brain injury and therefore subsequent brain changes are visible in conventional MRI sequences.[21-23,31,32] Hyperperfusion evidenced in this dog affected by CLN is consistent with findings reported in an experimental study, where hyperperfusion of compromised brain areas was detected 1 week after induced ischemic events in Beagle dogs.[33]

Perfusion values in the apparently normal brain parenchyma in the left hemisphere of the dog that suffered the consequences of brain hypoxia were comparable to the control dog CBF values (Table 1). On the other hand, CBF values in the current case report are lower compared to other reports where dynamic susceptibility contrast-enhanced PWI technique was used.[33-35] Although CBF is an absolute value, the CBF measurement method could have an influence, as our acquired values were most similar to the values obtained in the study where pCASL method was also used.[36] Second, different anesthesia protocols could have led to these discrepancies.[37]

In the current case report, blood pressure was not monitored during anesthesia used for the dental procedure. Hypotension (mean arterial blood pressure <60 mm Hg or systolic blood pressure <80 mm Hg) is 1 of the most common anesthetic complications in veterinary medicine, occurring in about 38% of anesthetized dogs.[38] In human medicine, cortical blindness is mainly described in patients undergoing coronary bypass artery grafting procedures (55%) and in thoraco-vascular surgery (23%).[39] Although etiology of cortical blindness is not entirely understood in these patients, hypotension was found in 45% of the reported cases.[39] Unrecognized hypotension could have been the cause of cerebral hypoperfusion and subsequent cortical necrosis in this dog.

The main limitation of the current case report is the absence of the postmortem examination, precluding correlation between MRI and histopathological findings in the dog suffering from CLN.

Identification and characterization of CLN using 3-Tesla MRI and PWI might contribute to new treatment strategies in dogs suffering the consequences of cerebral hypoxia.

ACKNOWLEDGMENTS

The authors are grateful to the Stiftung Kleintiere for providing the arterial spin labeling sequence. Parts of this report have been presented as a research abstract poster at the 31st annual symposium of the ESVN-ECVN, September 20-22, 2018, Copenhagen, Denmark.

CONFLICT OF INTEREST DECLARATION

Authors declare no conflict of interest.

OFF-LABEL ANTIMICROBIAL DECLARATION

Authors declare no off-label use of antimicrobials.

INSTITUTIONAL ANIMAL CARE AND USE COMMITTEE (IACUC) OR OTHER APPROVAL DECLARATION

Healthy beagle dog images archived from an independent research study were used as a control in the current case report. Animal permission number: ZH272/16.

HUMAN ETHICS APPROVAL DECLARATION

Authors declare human ethics approval was not needed for this study.

ORCID

Neringa Alisauskaite https://orcid.org/0000-0003-1820-4717
Adriano Wang-Leandro https://orcid.org/0000-0003-2991-5696

REFERENCES

1. Komiyama M, Nishikawa M, Yasui T. Cortical laminar necrosis in brain infarcts: chronological changes on MRI. *Neuroradiology*. 1997;39(7):474-479.
2. Siskas N, Lefkopoulos A, Ioannidis I, et al. Cortical laminar necrosis in brain infarcts: serial MRI. *Neuroradiology*. 2003;45(5):283-288. https://doi.org/10.1007/s00234-002-0887-7.
3. Tameemm A, Krovvidi H. Cerebral physiology. *Contin Educ Anaesthesia, Crit Care Pain*. 2013;13(4):113-118. https://doi.org/10.1093/bjaceaccp/mkt001.
4. Kinoshita T, Ogawa T, Yoshida Y, et al. Curvilinear T1 hyperintense lesions representing cortical necrosis after cerebral infarction. *Neuroradiology*. 2005;47(9):647-651. https://doi.org/10.1007/s00234-005-1398-0.
5. Takahashi S, Higano S, Ishii K, et al. Hypoxic brain damage: cortical laminar necrosis and delayed changes in white matter at sequential MR imaging. *Radiology*. 1993;189(2):449-456.
6. Samain JL, Haven F, Gille M, et al. Typical CT and MRI features of cortical laminar necrosis. *J Belgian Soc Radiol*. 2011;94(6):357. https://doi.org/10.5334/jbr-btr.713.
7. Sawada H, Udaka E, Seriu N, et al. MRI demonstration of cortical laminar necrosis and delayed white matter injury in anoxic encephalopathy. *Neuroradiology*. 1990;32(4):319-321.
8. Mariani CL, Platt SR, Newell SM, et al. Magnetic resonance imaging of cerebral cortical necrosis (polioencephalomalacia) in a dog. *Vet Radiol Ultrasound*. 2001;42(6):524-531.
9. Braund KG, Vandevelde M. Polioencephalomalacia in the dog. *Vet Pathol*. 1979;16(6):661-672. https://doi.org/10.1177/030098587901600604.
10. Khardenavis V, Karthik DK, Kulkarni S, et al. Cortical laminar necrosis in a case of migrainous cerebral infarction. *BMJ Case Rep*. 2018;2018:1-3. https://doi.org/10.1136/bcr-2017-221483.
11. Panarello GL, Dewey CW, Barone G, et al. Magnetic resonance imaging of two suspected cases of global brain ischemia. *J Vet Emerg Crit Care*. 2004;14(4):269-277.
12. Timm K, Flegel T, Oechtering G. Sequential magnetic resonance imaging changes after suspected global brain ischaemia in a dog. *J Small Anim Pract*. 2008;49(8):408-412. https://doi.org/10.1111/j.1748-5827.2008.00547.x.
13. Yoon-Soo J, Ili-Hwa K, Hyun-Gu K. Laminar cortical necrosis (polioencephalomalacia) caused by postoperative fluid overload in a dog with pyometra. *J Vet Clin*. 2017;34(2):98-102.
14. Thomsen BB, Gredal H, Wirenfeldt M, et al. Spontaneous ischaemic stroke lesions in a dog brain: neuropathological characterisation and comparison to human ischaemic stroke. *Acta Vet Scand*. 2017;59(7):1-9. https://doi.org/10.1186/s13028-016-0275-7.
15. Shimada A, Morita T, Ikeda N, et al. Hypoglycaemic brain lesions in a dog with insulinoma. *J Comp Pathol*. 2000;122(1):67-71. https://doi.org/10.1053/jcpa.1999.0342.
16. Howard RS, Holmes PA, Siddiqui A, et al. Hypoxic-ischaemic brain injury: imaging and neurophysiology abnormalities related to outcome. *QJM*. 2012;105:551-561. https://doi.org/10.1093/qjmed/hcs016.
17. Arbelaez A, Castillo M, Mukherji SK. Diffusion-weighted MR imaging of global cerebral anoxia. *Am J Neuroradiol*. 1999;20(6):999-1007.
18. Tha KK, Terae S, Yamamoto T, et al. Early detection of global cerebral anoxia: improved accuracy by high-*b*-value diffusion-weighted imaging with long echo time. *Am J Neuroradiol*. 2005;26(6):1487-1497. https://doi.org/10.1016/B978-0-240-80868-0.50004-8.
19. McKinney AM, Teksam M, Felice R, et al. Diffusion-weighted imaging in the setting of diffuse cortical laminar necrosis and hypoxic-ischemic encephalopathy. *Am J Neuroradiol*. 2004;25(10):1659-1665.
20. Kawahara H, Takeda Y, Tanaka A, et al. Does diffusion-weighted magnetic resonance imaging enable detection of early ischemic change following transient cerebral ischemia? *J Neurol Sci*. 2000;181(1–2):73-81. https://doi.org/10.1016/S0022-510X(00)00433-0.
21. Deibler A, Pollock J, Kraft RA, et al. Arterial spin-labeling in routine clinical practice, part 3: hyperperfusion patterns. *Am J Neuroradiol*. 2008;29(8):1428-1435. https://doi.org/10.3174/ajnr.A1034.
22. Haller S, Zaharchuk G, Thomas DL, et al. Arterial spin labeling perfusion of the brain: emerging clinical applications. *Radiology*. 2016;281(2):337-356. https://doi.org/10.1148/radiol.2016150789.
23. Wintermark P. Injury and repair in perinatal brain injury: insights from non-invasive MR perfusion imaging. *Semin Perinatol*. 2015;39(2):124-129. https://doi.org/10.1053/j.semperi.2015.01.005.
24. Donaire D, Carreno M, Gomez B, et al. Cortical laminar necrosis related to prolonged focal status epilepticus. *J Neurol Neurosurg Psychiatry*. 2006;77(1):104-106. https://doi.org/10.1136/jnnp.2004.058701.
25. Busl KM, Greer DM. Hypoxic-ischemic brain injury: pathophysiology, neuropathology and mechanisms. *NeuroRehabilitation*. 2010;26(1):5-13. https://doi.org/10.3233/NRE-2010-0531.
26. Weiss ATA, Graf C, Gruber ADD, et al. Leukoencephalomalacia and laminar neuronal necrosis following smoke inhalation in a dog. *Vet Pathol*. 2011;48(5):1016-1019. https://doi.org/10.1177/0300985810384412.
27. Oneil BJ, Koehler RC, Neumar RW, et al. Global brain ischemia and reperfusion. *Card Arrest Sci Pract Resusc Med*. 2007;27(5):236-281. https://doi.org/10.1017/CBO9780511544828.015.
28. Cervós-Navarro J, Diemer N. Selective vulnerability in brain hypoxia. *Crit Rev Neurobiol*. 1991;6(3):149-182.
29. Fortuna S, Pestalozza S, Lorenzini PBG. Transient global brain hypoxia-ischemia in adult rats: neuronal damage, glial proliferation, and

alterations in inositol phospholipid hydrolysis. *Neurochem Int*. 1997;31 (4):563-569.
30. Allen LM, Hasso AN, Handwerker J, et al. Sequence-specific MR imaging findings that are useful in dating ischemic stroke. *Radiographics*. 2012;32 (5):1285-1297. https://doi.org/10.1148/rg.325115760.
31. Pollock JM, Whitlow CT, Deibler AR, et al. Anoxic injury-associated cerebral hyperperfusion identified with arterial spin-labeled MR imaging. *Am J Neuroradiol*. 2008;29(7):1302-1307. https://doi.org/10.3174/ajnr.A1095.
32. Van den Brule JMD, Van der Hoeven JG, Hoedemaekers CWE. Cerebral perfusion and cerebral autoregulation after cardiac arrest. *Biomed Res Int*. 2018;2018:1-5.
33. Lu SS, Liu S, Zu QQ, et al. Multimodal magnetic resonance imaging for assessing lacunar infarction after proximal middle cerebral artery occlusion in a canine model. *Chin Med J (Engl)*. 2013;126(2):311-317. https://doi.org/10.3760/cma.j.issn.0366-6999.20121983.
34. Hartmann A, von Klopmann C, Lautenschläger IE, et al. Quantitative analysis of brain perfusion parameters in dogs with idiopathic epilepsy by use of magnetic resonance imaging. *Am J Vet Res*. 2018;79(4):433-442. https://doi.org/10.2460/ajvr.79.4.433.
35. Schmidt MJ, Kolecka M, Kirberger R, et al. Dynamic susceptibility contrast perfusion magnetic resonance imaging demonstrates reduced periventricular cerebral blood flow in dogs with ventriculomegaly. *Front Vet Sci*. 2017;4(137):5-7. https://doi.org/10.3389/fvets.2017.00137.
36. Chang FY, Xiao JX, Xie S, et al. Determination of oxygen extraction fraction using magnetic resonance imaging in canine models with internal carotid artery occlusion. *Sci Rep*. 2016;6(30332):1-8. https://doi.org/10.1038/srep30332.
37. Slupe AM, Kirsch JR. Effects of anesthesia on cerebral blood flow, metabolism, and neuroprotection. *J Cereb Blood Flow Metab*. 2018;38 (12):2192-2208. https://doi.org/10.1177/0271678X18789273.
38. Redondo JI, Rubio M, Soler G, et al. Normal values and incidence of cardiorespiratory complications in dogs during general anaesthesia. A review of 1281 cases. *J Vet Med Ser A Physiol Pathol Clin Med*. 2007;54(9):470-477. https://doi.org/10.1111/j.1439-0442.2007.00987.x.
39. Roth S, Miller RD. *Postoperative Visual Loss*, *Miller's Anesthesia*. 7th ed. New York, NY: Elsevier; 2010:2821-2841.

How to cite this article: Alisauskaite N, Wang-Leandro A, Dennler M, et al. Conventional and functional magnetic resonance imaging features of late subacute cortical laminar necrosis in a dog. *J Vet Intern Med*. 2019;33:1759–1765. https://doi.org/10.1111/jvim.15526